Stability and connectivity of real foodwebs predicted by mass constraints on maximum consumption and density dependence

Tianyun Lin[1] | tlin56@ucla.edu

Daniel J. Wieczynski[2,3] | daniel.wieczynski@duke.edu

Van M. Savage[1,3,4*] | vsavage@ucla.edu

[1]*Department of Computational Medicine, University of California at Los Angeles, Los Angeles, California 90095, USA.*

[2]*Department of Biology, Duke University, 130 Science Drive, Durham, NC 27708, USA.*

[3]*Department of Ecology and Evolutionary Biology, University of California at Los Angeles, Los Angeles, California 90095, USA.*

[4]*Santa Fe Institute, Santa Fe, New Mexico 87501, USA.*

[*]Corresponding Author: Van M. Savage | UCLA, Department of Ecology and Evolutionary Biology, Box 951766, Los Angeles, CA 90095 USA | Telephone: +1(310)206-6692 | Fax: 310-432-5012 | E-mail: vsavage@ucla.edu

Running Title: Body size predicts foodweb stability & links

Keywords: Body size, consumption rate, density dependence, connectance, foodweb stability.

Type of article: Letter

Number of words: 150 (abstract) and 4961 (main text)

Number of references: 57

Number of figures: 4; **Number of tables:** 1

Authorship: Conceptualization: T.L. and V.S.; theory development: T.L. D.W., and V.S.; theoretical and numerical analysis: T.L.; results interpretation: T.L., D.W., and V.S.; writing: T.L., D.W., and V.S.

Data accessibility statement: We confirm that, should the manuscript be accepted, the data supporting the results will be archived and available in the Figshare Repository and the data DOI will be included at the end of the article.

ABSTRACT

Understanding which foodwebs thrive or collapse is a major challenge that has been mostly studied in terms of topology and interaction strength. Yet the relative importance of these properties is hotly debated due to limited research on how they interact and which forces generate them. Here, we construct a foodweb model that incorporates mass-based constraints on density dependence, maximum consumption rate, and the likelihood and strength of interactions, which in turn control overall topologies and interaction strength distributions. Our model predicts both stability and connectivity that closely match real foodwebs ranging widely in size (29-163 species) and connectivity (113-1086 interactions). Despite their absence in most research, density dependence and maximum consumption rate are not only required to accurately predict stability but have stronger impacts than the more-frequently-studied interaction strength. Our results demonstrate that predicting foodweb stability requires simultaneously considering multiple foodweb properties—all of which naturally emerge from species masses.

INTRODUCTION

From vast grasslands in northern Europe to lush tropical forests in southeast Asia, nature has created foodwebs of different sizes, structures, and complexity. Scientists have long worked to gain a better understanding of which properties of foodwebs determine their persistence and stability (Elton 1927; May 1973; Emmerson & Raffaelli 2004; Stouffer & Bascompte 2011; Tang & Allesina 2014). Traditionally, ecologists argued that complex foodwebs are more stable than simple foodwebs because of redundancy and robustness (Odum 1953; MacArthur 1955; Paine 1966). Then Robert May showed that larger and more complex systems are less stable for

53 the simplest scenario of random species interactions (May 1972). Such conflicting views have
54 given rise to the stability-complexity debate for foodwebs (Landi *et al*. 2018).
55
56 Theorists frequently explore how trophic interaction strengths and foodweb topology—
57 connectance, modularity, nestedness—individually affect foodweb stability. The consensus is
58 that both play crucial roles (Brose *et al.* 2006; Grilli *et al.* 2016). Specifically, several studies
59 showed that modularity is positively correlated with foodweb stability (Stouffer & Bascompte
60 2011; Grilli *et al.* 2016), which is based on the reasoning that a disturbance within a subgroup is
61 less likely to propagate to the rest of the foodweb when modularity is high. In contrast, trophic
62 interaction strength has been shown to negatively correlate with foodweb stability (Emmerson &
63 Raffaelli 2004) because weaker interactions reduce oscillations in consumer-resource
64 abundances (McCann *et al.* 1998).
65
66 So far, most researchers have studied foodweb topology and interaction strength independently.
67 For instance, when studying the effect of foodweb topology on stability, researchers often
68 sample consumer-resource interaction strengths randomly from a distribution with zero mean
69 and a variance of one (May 1972; Grilli *et al.* 2016). This stands in contrast to real systems for
70 which it is empirically well-known that trophic interaction strengths are correlated with and
71 bounded by metabolic rate, attack rate, handling time, etc. (Pawar *et al.* 2012). In addition, when
72 studying the effect of interaction strength on stability, trophic links are typically placed randomly
73 within the foodweb (May 1972; Tang *et al.* 2014), ignoring the fact that real webs have non-
74 random topology and are structurally anti-symmetric (Chawanya & Tokita 2002). To circumvent
75 this, foodweb topology is sometimes estimated from empirical data such that there is no topology

76 generating mechanism in the model (Emmerson & Raffaelli 2004). Other times interaction
77 strength is studied through small trophic modules that only consist of 3 to 4 species (McCann *et*
78 *al*. 1998), which avoids the large foodweb structure.
79
80 Indeed, isolating individual factors can make them easier to study. However, such an approach
81 often misses important interactions or correlations among factors that are present in real systems.
82 Consequently, a model that describes nature—by accurately inferring foodweb stability—most
83 likely needs to incorporate both ecologically informed topology and trophic interaction strengths.
84 It has been challenging to link models and theory outputs sensibly with empirical foodwebs,
85 partly because we lack a natural or parsimonious way to link topological properties and
86 interaction strength. Here, we argue that species mass is a remedy for this issue.
87
88 Species body mass has been previously used as a constraint on both foodweb topology and
89 trophic interaction strengths (Cohen *et al.* 1993; Pawar *et al.* 2012). Trophic interaction strength
90 is generally defined as the rate at which a consumer feeds on a resource (Mittelbach & McGill
91 2019). It thus depends on the densities of consumers and resources as well as consumer-resource
92 traits such as search rate, attack rate, and handling time of the consumer. Several studies have
93 shown that these traits scale with the body masses of consumers and resources through allometric
94 scaling (Brose 2010; Pawar *et al.* 2012; Brose *et al.* 2006; Gillooly *et al.* 2001).
95
96 Mass constraints on topological properties, however, are more subtle. The cascade model was
97 used in early research on size-structured foodwebs (Cohen *et al.* 1993). A core assumption of the
98 cascade model is equiprobability (Neubert *et al.* 2000)—consumers only interact with smaller

resources and there is an equal probability of any single smaller species being used as a resource. However, previous empirical studies have shown that consumers prefer resources of certain sizes and that the trophic interactions are limited by the slow movement of consumers and longer reactive distances when consumer-resource body size-ratios are large (relatively larger prey or smaller predator). Conversely, small size-ratios are limited by a consumer's ability to detect and catch small prey (Thiebaux & Dickie 1993; Hansen *et al.* 1994; Brose *et al.* 2008; Brose 2010). Thus, it is crucial for a foodweb model to implement an interaction likelihood that is hump-shaped with respect to consumer-resource size-ratios (Pawar *et al.* 2019).

Although mass constraints on topology and interaction strength have been investigated, there has been very little effort in foodweb stability analysis to investigate or include species mass constraints on two other key foodweb properties: 1) density dependence and 2) maximum consumption rate. Previous studies often either set all species' density dependence to -1 (May 1972) or ignore density dependence altogether (Grilli *et al.* 2016). However, there is substantial evidence from empirical studies on foodwebs that species commonly experience density dependence (Brook & Bradshaw 2006; Woiwod & Hanski 1992). And more importantly, density dependence is highly related to species abundance, which in turn scales with species mass (Damuth 1981; Yeakel & Redner 2018). Therefore, we can incorporate density dependence into foodweb models by using species masses to estimate density dependence intensity and empirical data to approximate the percentage of species that experience density dependence.

Maximum consumption constraint—an upper limit on each consumer's total energy intake (total consumption rate)—arises because an organism cannot consume limitless resources. A

consumer's diet is affected by factors such as resource abundance, attack probability, capture success rate (Manly 1974 & Chesson 1978, 1983), predation risk (Ho *et al.* 2019), and gape-limitation (Hairston & Hairston 1993), all of which can be determined by species body mass and C-R mass-ratio (Pawar *et al.* 2012). Because species mass limits maximum consumption rate (Damuth 1981; Pawar *et al.* 2012; Ho *et al.* 2019), the total amount of resource that can be consumed is constrained. Therefore, this mass-constrained diet places a limit on the number of resource links (the rate of consumption of each resource) for each consumer species and governs the connectance of the whole foodweb and ultimately affects their stability (May 1972; Dune & Williams 2009).

Most models have ignored the size constraint of density dependence and any effect of maximum consumption. We argue that these omissions have likely led to misestimation of foodweb stability and connectance. Here, we construct a comprehensive model based on generalized Lotka-Volterra framework in which realistic values for key network properties—trophic topology, interaction strength distributions, foodweb modularity, and connectance—emerge naturally from species masses and mass-constrained density dependence and maximum consumption. Thus, our novel framework can be used to realistically predict network properties and foodweb stability based only on species masses. In so doing, we clarify the origins and pervasiveness of the foodweb complexity-stability relationship. Furthermore, by changing the model assumptions to include or omit the size-dependence of the four main factors—interaction likelihood, interaction strength, density dependence, and maximum consumption—we disentangle the individual and combined effects of key ecological constraints on foodweb stability.

Model Development

Allometric Regulation Trophic Model (ART Model)

Here, we describe the steps and procedure of the Allometric Regulation Trophic (ART) model framework, which constructs foodwebs (similar to interaction matrix derived from generalized Lotka-Volterra model) from the ground up using realistic mass-based constraints on species composition and consumer-resource pairing (see Supplementary Information section 1 & Fig. S3 for more details):

Step 0. **Species mass:** To start building the foodweb, n species are chosen with masses $m_1, m_2, \dots, m_n$ sampled from a lognormal distribution with mean μ_m and variance σ_m^2 (Supporting Information section 1.1).

Step 1. **Interaction likelihood & trophic links:** For all pairwise trophic interactions (consumer *i* and resource *j*), the interaction likelihood is $\mathcal{L}_{ij} = g(\frac{m_j}{m_i}|\mu_l, \sigma_l^2)$ for all $i = 1, 2, \dots, n$, $j = 1, 2, \dots, n$, and $i \neq j$. Note that the function g is a lognormal PDF of consumer-resource mass-ratio and μ_l and σ_l^2 are the mean and variance of the C-R mass-ratio distribution (Supporting Information section 1.2). For all trophic links, pick the p% ($p \leq \frac{n^2-n}{2n^2}$) of consuming links (flow from resource to consumer) with highest interaction likelihood (Fig. 1a). Then the number of selected links is $\kappa = n^2 \cdot \frac{p}{100}$ (rounded to the nearest integer if necessary). Moreover, each selected link ($SL = \{l_1, l_2, \dots, l_\kappa\}$) is a set of two numbers, i.e. $l_k = (i, j)$, that describes a consumer (i) feeding on a resource (j). Note that

for each trophic link selected, the associated resource link (flow from resource out to consumer) for the pair is also selected. Thus, the total percentage of links selected from the entire web is actually $2p$.

Step 2. **Interaction strength:** Calculate the interaction strength for all selected trophic links using metabolic theory and the masses of resources and consumers (Fig. 1b). Specifically, for consumers and resources with masses m_C and m_R, respectively, the per-capita consumption rate (α_R) of resource by consumer can be calculated as a measure of interaction strength:

$$\alpha_R = -\frac{sAf}{m_C} \tag{1}$$

which is comprised of search rate (s) (on a per-capita and per-area basis), attack success probability (A), consumer biomass (m_C), and functional response (f) that can be type I, II, or III (Holling 1959; Jeschke *et al.* 2004; Vucic-Pestic *et al.* 2010). We use type I functional response that depends on resource abundance (R) because of its simplicity and the results produced by type I and II functional response are qualitatively the same (Fig. S5). Thus, we can construct a mass-constrained interaction matrix (I):

$$I_{ij}\ (\text{area per mass per time}) = e \cdot \frac{s_{ij}A_{ij}f_{ij}}{m_i} \tag{2}$$

where I_{ij} is calculated if (i, j) is a selected link belonging to SL. The corresponding $I_{ji} = -\frac{s_{ij}A_{ij}f_{ij}}{m_i}$, *thus imposing a structural type of anti-symmetry to the foodweb matrix*. All other links are zero. Note that s_{ij}, A_{ij}, and f_{ij} depend on the masses and mass-ratios of consumer i and resource j.

Step 3. **Maximum consumption:** Using the interaction matrix, for each species we calculate the total consumption rate, i.e. $T_i = \sum_{j=1}^{n} I_{ij}$ for $I_{ij} > 0$ (restricting the sum to only terms that involve consumption for species i). If the total consumption rate of a species exceeds its metabolic rate, i.e. $T_i > z_0 m_i^{0.75}$ (Supporting Information section 1.3; Fig. S2; Kleiber 1947), the model "prunes" excessive trophic interactions by randomly setting one of the consumption rates to zero (Fig. 1c). We repeat this process until $T_i \leq z_0 m_i^{0.75}$ for all i. Note that the selection process is chosen to be random because the interaction likelihoods of each consumer-resource pair are already similar after the first weighted sampling of interactions in step 2. In addition, because species diet choice is affected by a complex set of factors, random selection is the least biased method.

Step 4. **Density dependence:** Certain species with dense populations may experience density dependence (intraspecific competition) (Brook & Bradshaw 2006), which has a strong stabilizing effect on foodweb dynamics (Barabás *et al.* 2017). The density dependence intensity for each species is calculated as the ratio between species growth rate (r) and carrying capacity (K), i.e. r/K. This term results from a standard logistic growth function that leads to sigmoidal growth with an asymptotic upper limit set by the carrying capacity and directly related to intraspecific competition within species (Yodzis & Innes 1992; Weitz & Levin 2006). In addition, since both growth rate and carrying capacity scale with mass (Pawar *et al.* 2012), the mass-scaling for density dependence intensity combines to be $(r_0/K_0)m^{-0.5}$, where r_0 and K_0 are the respective scaling constants for growth rate and carrying capacity (Pawar *et al.* 2012). After calculating density dependence for all species, select q% (Supporting Information section 1.4) of species with the highest

density dependence values and assign these as the diagonal terms in the interaction matrix. Density dependence for the remaining species is set to zero (Fig 1d).

The final interaction matrix formed from all of these steps is referred to as $\tilde{I}$. Consequently, our ART foodweb model creates networks where the directed edges/links between nodes (species) represent mass-based feeding behavior, i.e. diet. The weight (thickness) of the edge represents the trophic interaction strength (Fig 1).

In short, the ART Model incorporates mass-based effects on interaction likelihood, interaction strength, maximum consumption, and density dependence as four core components. Note that even though all these components are determined by mass, they can be analyzed independently. Hence, a big advantage of the ART Model is that it can easily disentangle effects and interactions among these four potentially important factors. By including or omitting one or more core components, we create five different mass-based foodweb models (Fig. 2) that represent a range of model classes. In so doing, we can understand the individual or combined effects of each component on foodweb stability:

(1) **Random Model (RM):** For this model, the trophic interactions are placed randomly. Each interaction strength is randomly sampled from a uniform distribution with mean and range constrained by the mean and range of species mass (Supporting. Information section 2). The diagonal terms of the interaction matrix are all -1, corresponding to strong density dependence for all species. Note that the RM omits all four core components and is analogous to the “Random” Foodweb created and analyzed in May’s original paper on the complexity-stability debate (May 1972).

(2) **Base Mass Model (BMM):** This model only includes steps 0-2 of the ART model and excludes steps 3 and 4, which means no maximum consumption or density dependence, i.e. all entries are -1 on diagonal and no positive row-sum constraint for the interaction matrix.

(3) **Base + Density Dependence Model (BDDM):** This model includes steps 0-2, and density dependence (step 4) of the ART model but excludes the maximum consumption constraint (step 3).

(4) **Base + Maximum Consumption Model (BMCM):** This model includes steps 0-3 of the ART model but excludes density dependence (step 4).

(5) **ART Model:** Includes all steps 0-4 and all core components.

MATERIALS AND METHODS

Stability analysis

For each model foodweb, stability is defined by whether a foodweb eventually returns to its original state of species abundances after perturbation (a change in one or more abundances for any reason). This is mathematically determined by calculating the eigenvalues of the interaction matrix (Jacobian), i.e.

$$J(X^*) = \tilde{I} \tag{3}$$

to determine whether the eigenvalues are all negative, meaning the perturbed abundances will all exponentially decay back to their original state, or whether at least one eigenvalue is positive, meaning at least one perturbed abundance will exponentially grow, never return to its original state, and the system is defined as unstable (May 1972; Otto & Day 2011; Allesina & Tang

2015). Note that the Jacobian matrix is equivalent to the interaction matrix in our case because the foodweb dynamics is based on the generalized Lotka-Volterra model; and in addition, we are assuming and only interested in non-trivial solutions (abundance is non-zero for all species). Thus, taking the derivative of our model gets rid of the dependence on the species abundance column vector (Supporting Information section 1.2).

For all models and for each choice of parameters, we compute the proportion of resulting networks that are stable—termed the frequency of stability—by simulating 1000 replicate networks for each parameter set, counting the number of cases where the real part of the leading eigenvalue is negative, and dividing this by the total number of repetitions (1000). In order to investigate how foodweb connectance, modularity, and interaction strength (Fig. 3) affect the frequency of stability, we vary the community mean consumer-resource mass-ratio (μ_l). That is, we vary the average resource mass preferred by consumers—higher μ_l indicates that consumers prefer larger resources. This allows us to compare and contrast our empirical consumer-resource mass-ratio distribution with model frequency of stability distributions across a range of possible average mass-ratios (μ_l) for all models. A high frequency of stability value implies that a given mean consumer-resource mass-ratio (μ_l) is favored in real foodwebs. Therefore, we expect the shape of the frequency of stability distribution to match empirical consumer-resource mass-ratio distributions (Supporting Information section 5).

Network properties of model foodwebs

To compare and contrast models with different assumptions, we also measure the connectance, modularity, and interaction strength for all models while varying mean consumer-resource mass-ratios (μ_l). Connectance is defined as the ratio between the number of observed trophic links and total possible trophic links (n^2) (Delmas *et al.* 2019). For modularity, we use a fast algorithm developed by Newman, which measures the degree of nodes connecting to nodes within the same group/cluster compare to other group (Newman 2004). The mean and variance of interaction strength distributions are calculated from all the positive entries of the interaction matrix. The connectance of the ART model is also calculated for different foodweb sizes.

Empirical data and parameters used for model comparison

For all model configurations and simulations, we initialize foodwebs with 93 species, corresponding to the average size of the eight empirical foodwebs for which we have comprehensive data for consumer-resource pairs and species masses (Table 1). Moreover, the initial connectance ($\frac{p}{93^2}$) of all model foodwebs (size = 93) is approximated from 189 empirical foodwebs, i.e. 8 foodwebs with species mass (Table 1) and 181 binary foodwebs (Cohen 2010). Note that the binary foodwebs only contain information on whether a consumer interacts with a resource (1 for interaction and 0 for no interaction). Therefore, these binary webs can be only used for estimating connectance.

Because each species in the 8 foodwebs with species mass information is identified and distinguished by its body mass and both the species mass and C-R mass-ratio distributions are typically unimodal (Fig. 2&S1), we obtain the mean and variance, i.e. μ_m and σ_m^2, used for

296 sampling species masses from the log-transformed species mass distributions of those 8
297 foodwebs. Similarly, we obtain the mean and variance—μ_l and σ_l^2—from the log-transformed
298 consumer-resource mass-ratio distributions of these empirical foodwebs to determine interaction
299 likelihood. These empirical foodwebs include Eastern Weddell Sea, Grand Cariçaie Marsh,
300 Scotch Broom, Skipwith Pond, Broadstone Stream, UK Grassland, Gearagh Woodland, and
301 Estero de Punta Banda (Pawar *et al.* 2019).
302
303 For conversion efficiency (e), Lindeman (1942) indicated that the efficiencies ranges from 0.001
304 to 0.375 based on the observation on energy transfer from one trophic level to the next. But later
305 research showed that e also differs across metabolic groups—herbivore, endotherms, ectotherms,
306 etc. (Peters 1986) and have higher values that range from 0.50 to 0.85 (Pawar *et al.* 2019).
307 Therefore, we simulate the ART model using efficiency ranges from 0.10-0.85 to test the impact
308 of efficiency on foodweb stability (Supporting Information section 6.2).
309
310 **RESULTS**
311
312 Because foodwebs that are stable and feasible should persist longer, the consumer-resource
313 mass-ratios associated with these webs should occur with higher frequency in nature (Borrelli *et*
314 *al.* 2015). From this perspective peak stability should occur at a mean interaction likelihood (μ_l)
315 that is close to the mean of empirical consumer-resource mass-ratio distributions. Indeed, the
316 ART model—which incorporates mass-based constraints on both maximum consumption and
317 density dependence—produces a frequency of stability distribution that peaks precisely at the
318 mean (around -1) of the empirical consumer-resource biomass-ratio distribution (Fig. 2).

More importantly, the frequency of stability decreases faster at higher consumer-resource mass-ratios and more gradually for lower ratios, matching these subtler features of the empirical consumer-resource biomass-ratio distribution. This is in strong contrast to other models that predict equal stability for those consumer-resource mass-ratio values (RM & BMM), and others that do not fully capture the shape of the empirical distribution (BDDM & BMCM). Intriguingly, this demonstrates that the mass-ratio lognormal distribution used for interaction likelihood sampling is not the only factor that determines the shape of the frequency of stability distribution.

Additionally, although weak interactions and strong correlations among the consumer-resource interactions (I_{ij} and I_{ji}) are known to improve stability (Emmerson & Raffaelli 2004; Tang *et al.* 2014) and correspond to real foodweb data (table 1), the ART model exhibits a peak in the frequency of stability at consumer-resource mass-ratios close to -1 (Fig. 2), which does not correspond with the weakest mean interaction strengths (Fig. 3b). Furthermore, the ART model correctly predicts poor stability for both small and large consumer-resource biomass-ratios, while mean interaction strength declines across the range (Fig. 3b). Taken together, these results suggest that interaction strength is not the strongest contributor to foodweb stability.

Conversely, we find that maximum consumption and density dependence constraints do play important roles in modulating the stability of foodwebs, as evidenced by the observation that the frequency of stability curves produced by the Random Model (RM) and Base Mass Model (BMM) do not match the empirical mass-ratio distribution. Both RM and BMM generates

uniform stability across mass-ratio, whereas the empirical distribution is lognormal (Fig. 2). Note that the stability values produced by BMM are all 1 due to stabilizing effect of correlation between trophic interaction pairs (Tang *et al.* 2014).

Moreover, maximum consumption and density dependence have divergent effects on foodweb stability (Fig. 2). Most notably, the frequency of stability curve produced without maximum consumption shifts the peak towards smaller C-R mass-ratios compared with the ART model. For the model with no density dependence, the peak for maximum stability matches the peak of the empirical C-R mass-ratio distribution (Fig. 2). This result indicates that the mass-based maximum consumption constraint is essential for correctly predicting the location of the peak of foodweb stability within the consumer-resource mass-ratio space.

Apart from stability, we discover that, as a mechanistic mass-based model, the ART model also more accurately captures the trends for how connectance (C) changes with foodweb size (n) empirically (Fig. 4), compared to other phenomenological models. Previously, Schmid-Araya *et al.* (2002) found that disagreeing with link-species "law", i.e. $C \sim n^{-1}$ (Hall & Raffaelli 1993), and constant connectance hypothesis, i.e. $C \sim n^{0}$ (Martinez 1992), the exponent for $\log(C)$ and $\log(n)$ should be close to -0.7, i.e. $C \sim n^{-0.7}$, by fitting a phenomenological model through extensive empirical data. The ART model produces exponent for $\log(C)$ and $\log(n)$ close to -0.7, i.e. $C \sim n^{-0.86}$, and outperforms link-species "law" and connectance hypothesis, which strengthens the ART model validity because foodwebs of different sizes (especially smaller foodwebs) often have drastically different connectances (Fig. 4) that play crucial roles in foodweb function and stability (May 1972; Landi *et al.* 2018).

In addition to connectance, modularity was also measured for each simulation as a metric of topology. Previous papers (Stouffer & Bascompte 2011; Grilli *et al.* 2016) suggested that modularity promotes stability by limiting the likelihood of collapse. Indeed, we find a high correlation between modularity and stability (Fig. 2&3c).

DISCUSSION

Understanding and separating how different foodweb properties—such as connectance, modularity, and interaction strengths—relate to the stability of foodwebs is a central challenge that has puzzled ecologists for decades (Elton 1958; Paine 1966; May 1972; Emmerson & Raffaelli 2004). We argue this has been puzzling largely due to the lack of models that include mechanistic processes that influence foodweb topology, interaction strength, density dependence, and maximum consumption simultaneously.

Therefore, by using species mass as a common currency that connects multiple aspects of foodweb properties, we create the ART Model that predicts foodweb stability—in terms of matching stability and connectance of empirical webs—better than all other model configurations that we consider. We show that foodweb topology is crucial for determining overall system stability (Fig. 3a), while interaction strength plays a relatively minor role (Fig. 3b). More precisely, we demonstrate that maximum consumption and density dependence are fundamental building blocks of foodweb topology that in turn lead to a more mechanistic and systematic understanding of how foodweb structure affects stability (Fig. 2&3).

Maximum consumption affects foodweb stability by limiting connectance and optimizing size-ratio based foraging strategies. More concretely, even though the allometrically scaled function (Eq. 1&2) can produce realistic interaction strengths for pairwise consumer-resource interactions, consumers normally feed on multiple resources to maximize their energy intake (Stephens & Krebs 1986). However, according to metabolic theory there is a mass-dependent upper bound for the total energy and rate of intake for each consumer. The ART model achieves the upper bound by omitting excessive trophic links. Fewer links leads to higher stability (Fig. 2&3a). The effect of maximum consumption on stability is distinguished by examining the BMCM. *And interestingly, we found that the BMCM exhibits a peak around consumer-resource mass-ratio close to 0, which indicates that a foodweb can be stable without any density dependence (Fig. 2).* This type of stability and the corresponding peak are achieved mainly by reduced connectance.

Although the ART model correctly predicts the trend for foodweb connectance, the absolute values of connectance are a little lower than empirical values (Fig. 4). A possible reason for systematically lower connectance is that the trophic links are collected accumulatively. Meaning that the empirical foodweb is not a "snapshot" but an overlay of "snapshots". Another reason is due to the fact that our maximum consumption constraint eliminates excessive trophic links instead of reducing their strengths. However, a recent study (Ho *et al.* 2019) suggests that predation risk constrains diet choice by weakening the existing trophic links instead of omitting links. Therefore, combining this "weakening" procedure with our "pruning" procedure in future models might further improve estimation of absolute values for connectance.

411

412 Density dependence can also strongly influence foodweb stability, yet studies often ignore the
413 size-dependence of density dependence. When constructing an interaction matrix, researchers
414 often set the diagonal terms (density dependence terms) to either all zeros or all negative ones.
415 The former case can be useful if only interested in how trophic interaction strengths or
416 correlations affect stability because setting diagonal terms to zero eliminates additional effects
417 from density dependence (Tang *et al.* 2014). However, this ignores the stabilizing effect of
418 density dependence and underestimates foodweb stability. The other common choice—setting
419 diagonal terms to all negative ones—imposes strong homogeneous regulation and artificially
420 inflates baseline stability in the system (May 1972).

421

422 From an ecological standpoint, it is unrealistic to assume that none of the species experience
423 density dependence in a foodweb. In nature, species often experience some form of density
424 dependence through intraspecific competition (Brook & Bradshaw 2006). By excluding
425 maximum consumption constraint, the BDDM produces two peaks around consumer-resource
426 mass-ratios close to -5 and 4. Although those stability peaks do not match the peak for empirical
427 mass-ratio distribution, the fact that stability moves away from preferred consumer-resource
428 mass-ratio indicates that when facing density dependence, species may choose resources with
429 unfavored biomass in order to survive and persist.

430

431 Besides maximum consumption and density dependence, an unexpected factor that also affects
432 foodweb stability in a rather complex way is conversion efficiency (Gibert & Yeakel 2019).
433 High conversion efficiency increases consumption rate but lowers connectance due to the

maximum consumption constraint. Low conversion efficiency reduces consumption rate but increases connectance. Interestingly, both cases behave similarly to the BDDM and exhibit stability peaks at mass-ratio close to -5 and 5 (Fig. S6). For ecological intuition, we speculate species may avoid competing for resources with preferred biomass and go for "unfavored" resources with high conversion efficiency. As for low efficiency, resources with preferred biomass would quickly die out and leave consumer with "unfavored" resources (Supporting Information section 6.2).

Based on our results, we argue that Random Matrix Theory (RMT) may not apply to empirical foodwebs. RMT assumes that networks are large and highly connected with random values occupying non-zero entries, producing an eigenvalue spectrum that is bounded by a circle (May 1972&1973; Allesina & Tang 2015) and with a well-defined boundary set by foodweb size and interaction strength. Nonetheless, the empirical foodwebs are normally small and sparsely connected (compare to unrealistic large values set by RMT) with trophic interactions that exhibit directional (energy/mass flow from resource to consumer) and non-random (constrained by species mass) patterns (Landi *et al*. 2018). Intriguingly, we find that a more realistic interaction matrix that is small, sparse, and non-random produces an eigenvalue spectrum with a shape closer to a diamond (boundary not well defined). We have not seen this diamond-shaped spectrum be previously reported (Fig. S7&8). The potential effects of this diamond-shaped eigenvalue spectrum on stability should be investigated in future research.

When looking at the predicted eigenvalue spectra for empirical foodwebs, the real parts of leading eigenvalues are close to or even exceed zero (Fig. S9), meaning that these empirical

457 foodwebs are not stable in the strict sense or may oscillate between stable and unstable states.
458 Such observations further suggest that we should shift from looking for absolute stability to
459 studying the frequency of stability and comparing other alternative metrics of stability
460 (Pettersson *et al.* 2019).
461
462 Throughout this project we tested our model with real data wherever possible. We argue that this
463 approach leads to crucial insights about the stability of foodwebs that were previously missed.
464 We used consumer-resource body mass-ratio distributions from eight well-measured empirical
465 foodwebs as a basis to predict foodweb stability. These predictions can be improved in the future
466 by incorporating more and larger foodweb datasets that include information about trophic links
467 as well as species masses. Future research should utilize more advanced tracking technologies
468 (Dell *et al.* 2014) and collect more comprehensive foodweb population abundance time-series
469 data to test model predictions.
470
471 In conclusion, we created a novel foodweb model termed ART that is solely driven by species
472 masses and that links all core foodweb characteristics—topology, interaction strength, maximum
473 consumption, and density dependence. Because of its flexibility and simple parameterization, the
474 ART model allows us to create sub-models and analyze how multiple ecological constraints
475 impact stability either alone or in combination. In doing so, we found that trophic interaction
476 strength distributions have a relatively weak impact on foodweb stability compared with the
477 energetic constraints of consumer maximum consumption and species density dependence.
478 Finally, our ART model correctly matches empirical patterns such as the frequency of stability

and connectance, a feat that to our knowledge has not been accomplished by other models (Landi. *et al*. 2018).

ACKNOWLEDGMENTS

We thank S. Pettersson, M. N. Jacobi, and P. Amarasekare for helpful discussion and comments on the manuscript. And we are grateful for funding from James F. McDonnell Foundation Complex System Scholar Award.

REFERENCES

Allesina, S., & Tang, S. (2015). The stability–complexity relationship at age 40: a random matrix perspective. *Popul. Ecol.*, *57*(1), 63-75.

Barabás, G., Michalska-Smith, M. J., & Allesina, S. (2017). Self-regulation and the stability of large ecological networks. *Nat. Ecol. Evol.*, 1(12), 1870-1875.

Borrelli, J. J., Allesina, S., Amarasekare, P., Arditi, R., Chase, I., Damuth, J., *et al*. (2015). Selection on stability across ecological scales. *Trends Ecol. Evol.*, 30(7), 417-425.

Brook, B. W., & Bradshaw, C. J. (2006). Strength of evidence for density dependence in abundance time series of 1198 species. *Ecology*, 87(6), 1445-1451.

Brose, U. (2010). Body-mass constraints on foraging behaviour determine population and food-web dynamics. *Funct. Ecol.* 24(1), 28-34.

499 Brose, U., Ehnes, R. B., Rall, B. C., Vucic-Pestic, O., Berlow, E. L., & Scheu, S. (2008).
500 Foraging theory predicts predator–prey energy fluxes. *J Anim. Ecol.* 77(5), 1072-1078.

501 Brose, U., Williams, R. J., & Martinez, N. D. (2006). Allometric scaling enhances stability in
502 complex food webs. *Ecol. Lett.* 9(11), 1228-1236.

503 Chawanya, T., & Tokita, K. (2002). Large-dimensional replicator equations with antisymmetric
504 random interactions. *J. Phys. Soc. Japan*, 71(2), 429-431.

505 Chesson, J. (1978). Measuring preference in selective predation. *Ecology*, 59(2), 211-215.

506 Chesson, J. (1983). The estimation and analysis of preference and its relationship to foraging
507 models. *Ecology*, 64(5), 1297-1304.

508 Cohen, J. E. (compiler) 2010. Ecologists' Co-Operative Web Bank. Version 1.1. Machine-
509 readable data base of food webs. New York: The Rockefeller University.

510 Cohen, J. E., Pimm, S. L., Yodzis, P., & Saldaña, J. (1993). Body sizes of animal predators and
511 animal prey in food webs. *J. Anim. Ecol.*, 67-78.

512 Damuth, J. (1981). Population density and body size in mammals. *Nature*, 290(5808), 699-700.

513 Dell, A. I., Bender, J. A., Branson, K., Couzin, I. D., de Polavieja, G. G., Noldus, L. P., ... &
514 Brose, U. (2014). Automated image-based tracking and its application in ecology. *Trends*
515 *Ecol. & Evol.*, 29(7), 417-428.

Delmas, E., Besson, M., Brice, M. H., Burkle, L. A., Dalla Riva, G. V., Fortin, M. J., ... & Olesen, J. M. (2019). Analysing ecological networks of species interactions. *Biol. Rev.*, *94*(1), 16-36.

Dunne, J. A., & Williams, R. J. (2009). Cascading extinctions and community collapse in model food webs. *Philos. T. R. Soc. B.*, 364(1524), 1711-1723.

Elton, C. S. (1927). *Animal Ecology*. Reprint 2001, University of Chicago Press, Chicago, IL.

Elton, C. S. (1958). *The ecology of invasions by animals and plants.* Chapman and Hall, London.

Emmerson, M. C., & Raffaelli, D. (2004). Predator–prey body size, interaction strength and the stability of a real food web. *J Anim. Ecol.*, 73(3), 399-409.

Gibert, J. P., & Yeakel, J. D. (2019). Eco-evolutionary origins of diverse abundance, biomass, and trophic structures in food webs. *Front. Ecol. and Evol.*, *7*, 15.

Gillooly, J. F., Brown, J. H., West, G. B., Savage, V. M., & Charnov, E. L. (2001). Effects of size and temperature on metabolic rate. *Science*, 293(5538), 2248-2251.

Grilli, J., Rogers, T., & Allesina, S. (2016). Modularity and stability in ecological communities. *Nat. Commun.*, 7, 12031.

Hairston Jr, N. G., & Hairston Sr, N. G. (1993). Cause-effect relationships in energy flow, trophic structure, and interspecific interactions. *Am. Nat.* 142(3), 379-411.

Hall, S. J., & Raffaelli, D. G. (1993). Food webs: theory and reality. In *Advances in ecological research* (Vol. 24, pp. 187-239). Academic Press.

Hansen, B., Bjornsen, P. K., & Hansen, P. J. (1994). The size ratio between planktonic predators and their prey. *Limnol. Oceanogr.*, 39(2), 395-403.

Ho, H. C., Tylianakis, J. M., Zheng, J. X., & Pawar, S. (2019). Predation risk influences food-web structure by constraining species diet choice. *Ecol. Lett*.

Holling, C. S. (1959). Some characteristics of simple types of predation and parasitism. *Can. Entomol.*, 91(7), 385-398.

Jeschke, J. M., Kopp, M., & Tollrian, R. (2004). Consumer-food systems: why type I functional responses are exclusive to filter feeders. *Biol. Rev.*, 79(2), 337-349.

Kleiber, M. (1947). Body size and metabolic rate. *Physiol. Rev.*, 27(4), 511-541.

Landi, P., Minoarivelo, H. O., Brännström, Å., Hui, C., & Dieckmann, U. (2018). Complexity and stability of ecological networks: a review of the theory. *Popul. Ecol*. 60(4), 319-345.

Lindeman, R. L. (1942). The trophic-dynamic aspect of ecology. *Ecology*, 23(4), 399-417.

MacArthur, R. H. (1955). Fluctuations of animal populations and a measure of community stability. *Ecology*, 36(3), 533-536.

Manly, B. F. J. (1974). A model for certain types of selection experiments. *Biometrics*, 281-294.

Martinez, N. D. (1992). Constant connectance in community food webs. *Am. Nat.*, *139*(6), 1208-1218.

May, R. M. (1972). Will a large complex system be stable?. *Nature*, 238(5364), 413.

May, R. M. (1973). *Stability and complexity in model ecosystems*. Princeton university press, Princeton, NJ

McCann, K., Hastings, A., & Huxel, G. R. (1998). Weak trophic interactions and the balance of nature. *Nature*, 395(6704), 794-798.

Mittelbach, G. G., & McGill, B. J. (2019). *Community ecology*. Second Edition. Oxford University Press, Oxford, United Kingdom, pp. 118-140

Neubert, M. G., Blumenshine, S. C., Duplisea, D. E., Jonsson, T., & Rashleigh, B. (2000). Body size and food web structure: testing the equiprobability assumption of the cascade model. *Oecologia*, 123(2), 241-251.

Newman, M. E. (2004). Fast algorithm for detecting community structure in networks. *Phys. Rev. E*, 69(6), 066133.

Odum, E. P. (1953). *Fundamentals of Ecology*. Saunders, Philadelphia, PA.

Otto, S. P., & Day, T. (2011). *A biologist's guide to mathematical modeling in ecology and evolution*. Princeton University Press.

Paine, R. T. (1966). Food web complexity and species diversity. *Am. Nat.* 100(910), 65-75.

Pawar S, Dell AI, Lin T, Wieczynski DJ and Savage VM (2019) Interaction Dimensionality Scales Up to Generate Bimodal Consumer-Resource Size-Ratio Distributions in Ecological Communities. *Front. Ecol. Evol.* 7:202.

571 Pawar, S., Dell, A. I., & Savage, V. M. (2012). Dimensionality of consumer search space drives
572 trophic interaction strengths. *Nature*, 486(7404), 485.

573 Peters, R. (1986). *The Ecological Implications of Body Size*. Cambridge: Cambridge University
574 Press.

575 Pettersson, S., Savage, V. M., & Nilsson-Jacobi, M. (2019). Predicting Collapse of Complex
576 Ecological Systems: Quantifying the Stability-Complexity Continuum. *bioRxiv*, 713578.

577 Schmid-Araya, J. M., Schmid, P. E., Robertson, A., Winterbottom, J., Gjerløv, C., & Hildrew, A.
578 G. (2002). Connectance in stream food webs. *J. Anim. Ecol.*, 1056-1062.

579 Stephens, D.W. & Krebs, J. (1986). Foraging Theory. Princeton Univ., Press. ISBN
580 9780691084428.

581 Stouffer, D. B., & Bascompte, J. (2011). Compartmentalization increases food-web persistence.
582 *Proc Natl Acad Sci U S A*, 108(9), 3648-3652.

583 Tang, S., Pawar, S., & Allesina, S. (2014). Correlation between interaction strengths drives
584 stability in large ecological networks. *Ecol. Lett.* 17(9), 1094-1100.

585 Thiebaux, M. L., & Dickie, L. M. (1993). Structure of the body-size spectrum of the biomass in
586 aquatic ecosystems: a consequence of allometry in predator–prey interactions. *Can. J.*
587 *Fish. Aquat. Sci.*, 50(6), 1308-1317.

588 Vucic-Pestic, O., Rall, B. C., Kalinkat, G., & Brose, U. (2010). Allometric functional response
589 model: body masses constrain interaction strengths. *J. Anim. Ecol.*, 79(1), 249-256.

590 Weitz, J. S., & Levin, S. A. (2006). Size and scaling of predator–prey dynamics. *Ecol. Lett.*, 9(5),
591 548-557.

592 Woiwod, I. P., & Hanski, I. (1992). Patterns of density dependence in moths and aphids. *J. Anim.*
593 *Ecol.*, 619-629.

594 Yeakel, J. D., Kempes, C. P., & Redner, S. (2018). Dynamics of starvation and recovery predict
595 extinction risk and both Damuth's law and Cope's rule. *Nat. Commun.*, *9*(1), 1-10.

596 Yodzis, P., & Innes, S. (1992). Body size and consumer-resource dynamics. *Am. Nat.*, 139(6),
597 1151-1175.

598 FIGURES

599

600 Figure 1

601

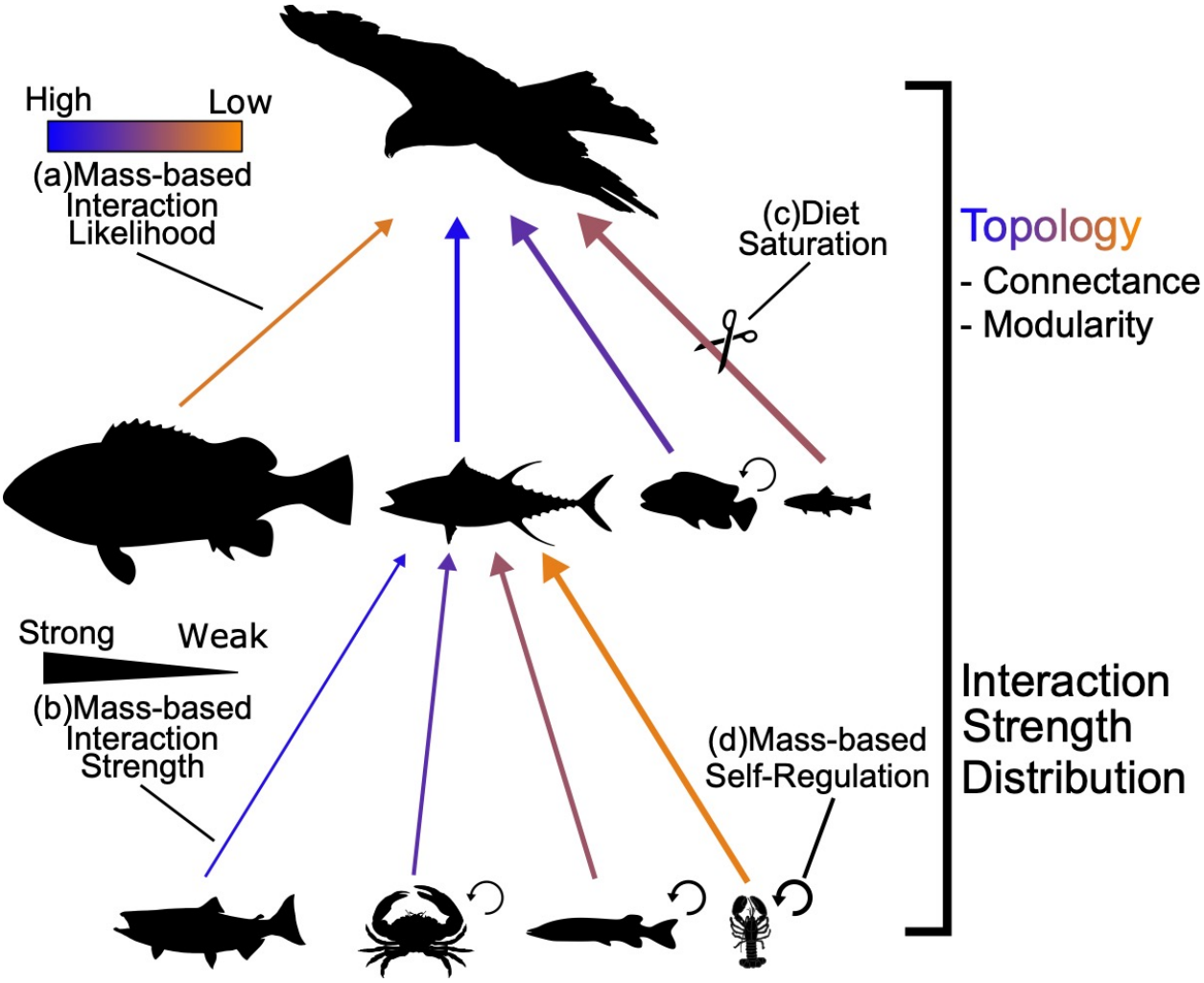

602

603 **Figure 2**

604

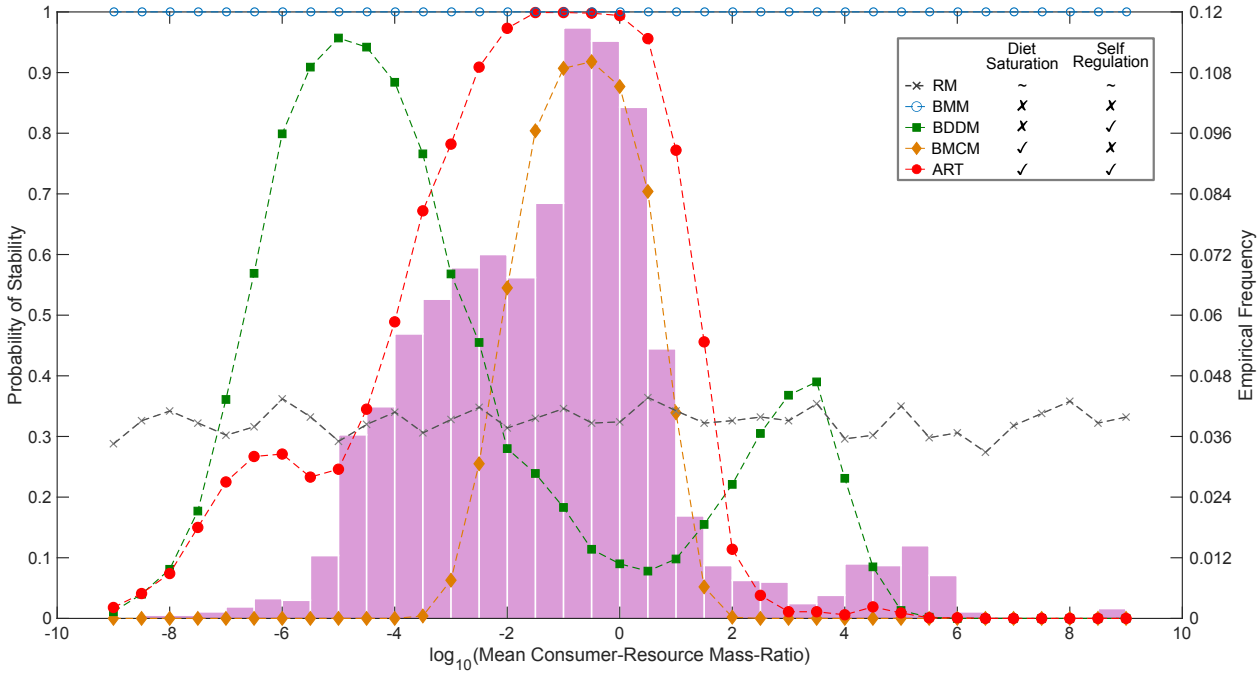

605

606 **Figure 3**

607

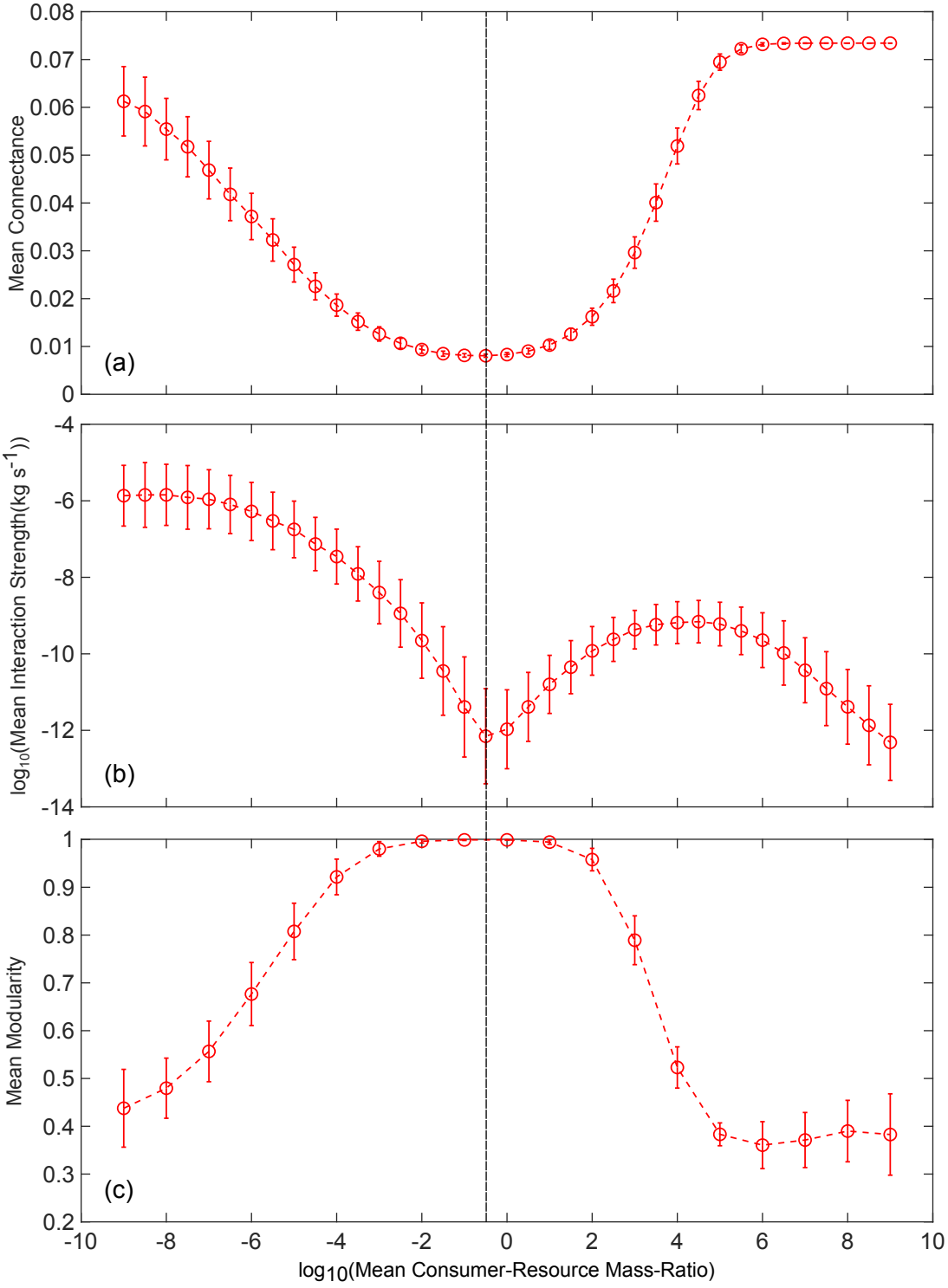

608

609 **Figure 4**

610

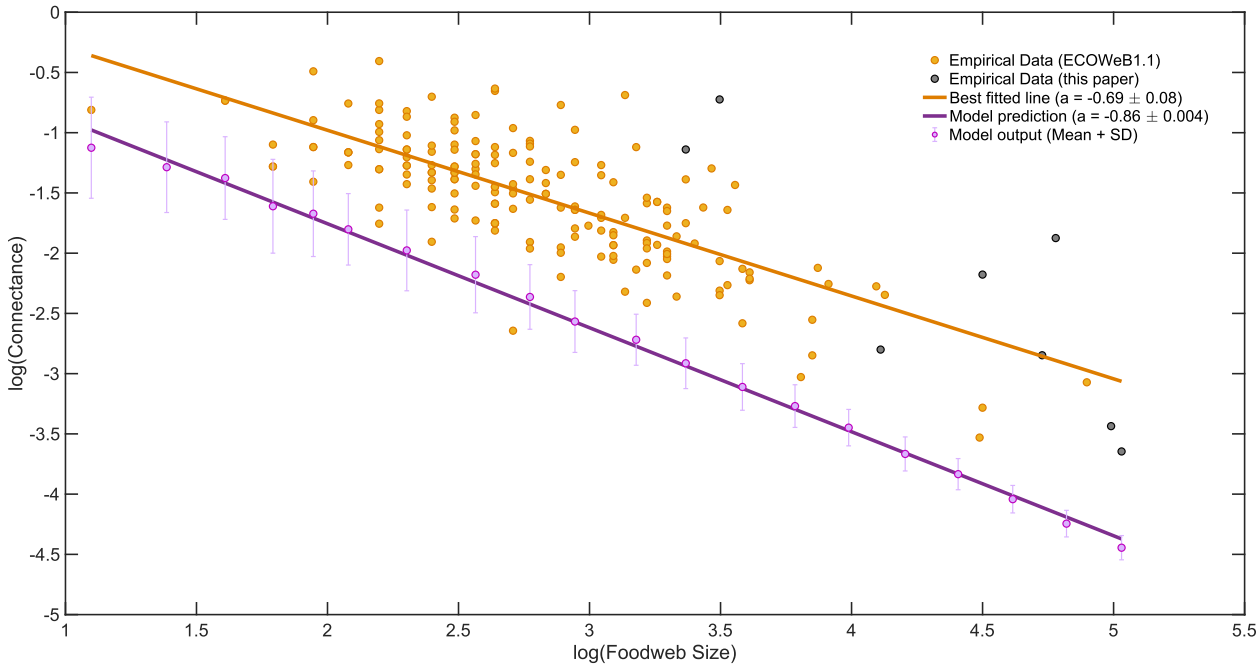

611

FIGURE CAPTIONS

Figure 1. Foodweb constructed by the ART Model. Generally, foodwebs consist of resource and consumer species as nodes. (a) Each trophic link/edge in the foodweb is assigned an interaction likelihood value (link color), which is a Gaussian function of log consumer-resource mass-ratios. (b) For each selected trophic link, the interaction strength (link width), i.e. consumption rate, is calculated using metabolic theory. (c) Maximum consumption rate constraint is imposed if the sum of all resource consumption rates (sum of all weighted trophic links) exceeds the maximum consumption rate for a given consumer. (d) Some species experience density dependence, the probability and strength of which both depend on mass. Note that topology is determined by interaction likelihood and diet while consumption rates and density dependence together shape the interaction strength distribution.

Figure 2. Stability results produced by our foodweb models compared with the empirical frequency of consumer-resource body mass-ratios. The empirical mass-ratio distribution was obtained from eight well documented foodweb datasets (Pawar *et al.* 2012). The frequency of stable foodwebs is shown for a variety of models. For the Random Model (RM), a fixed number of trophic links were selected randomly from a species pool with lognormally distributed masses. The Base Mass Model (BMM) is similar to RM except a fixed number of links were selected based on consumer-resource mass-ratio. Models with maximum consumption (BMCM) are built upon BMM by limiting the number of trophic links for each consumer species according to a mass-dependent maximum consumption rate. Models with density dependence (BDDM) are based on BMM as well by imposing a mass-based negative intraspecific density dependence on a subset of species (70%). Note that 70% is an average percentage of species experiencing density

636 dependence based on empirical data (Supporting Information section 1.4). The ART model
637 includes all features (steps 0-4 in main text). Note that the ART model produces a frequency of
638 stability that closely matches the empirical mass-ratio frequency.
639
640 **Figure 3.** Key network properties—(a) mean connectance (unitless, ranges 0-1), (b) log_{10}(mean
641 interaction strength (kg s^{-1})), and (c) modularity (unitless, ranges 0-1)—shown across a range of
642 consumer-resource mass-ratios for the ART foodweb model. All foodweb metrics represent
643 averages across 1000 replicate model simulations. And the error bars represent the standard
644 deviation for each data point. For interaction strength, the negative values are omitted since all
645 trophic pairs are perfectly correlated and the positive value equals the positive value times the
646 conversion efficiency constant.
647
648 **Figure 4.** Log-log plot for model and empirical foodweb connectance versus foodweb sizes. The
649 light orange points are connectance data of 181 foodwebs from ECOWeB1.1 compiled by Cohen
650 (2010). The grey points are connectance data of 8 foodwebs used in our paper. The orange line
651 represents the best fitted line for all empirical data (189 foodwebs) with slope $a = -0.69 \pm$
652 0.08. The light purple error bars represent the standard deviation of log(connectance) produced
653 by our ART model (over 200 run/foodweb size) over 15 different foodweb sizes. The dark purple
654 line represents the best fitted line for model connectance with slope $a = -0.86 \pm 0.004$. This
655 demonstrates that the ART model correctly predicts both stability properties and that the
656 connectance scales log-linearly with foodweb sizes. To our knowledge, the ART model is the
657 only size-based model to achieve this. Notably, the model predicts connectance values that are
658 always lower than the empirical data. This is possibly because empirical trophic links accumulate
659 and the maximum consumption constraint eliminates links instead of weakening them.

660 **Table 1.** Topological and allometric measurements for eight empirical foodwebs. The *Size*
661 column shows the number of trophic species in corresponding foodwebs. The *Connectance*
662 column measures the density of consumer-resource interactions (links) within foodwebs, i.e.
663 number of observed links over total possible number of links ($Size^2$). $log_{10}(mass)$ columns show
664 the observed mean (μ) and variance (σ^2) for log_{10} transformed species masses (kg). The
665 $log_{10}(m_R/m_C)$ columns show the observed mean (μ) and variance (σ^2) for log_{10} transformed
666 consumer-resource mass-ratios. The *Interaction Strength* columns measure the mean (μ) and
667 variance (σ^2) of the distributions of consumers' consumption rates (kg s^{-1}).
668

	Topology		log_{10}(mass)		$log_{10}(\frac{m_R}{m_C})$		*Interaction Strength*	
Foodwebs	*Size*	*Connectance*	μ	σ^2	μ	σ^2	μ	σ^2
Eastern Weddell Sea	153	0.0261	-2.85	5.13	-2.08	7.48	5.35E-05	3.24E-08
Grand Cariçaie Marsh	90	0.1133	-5.42	2.74	-0.68	2.61	6.51E-07	8.17E-11
Scotch Broom	147	0.0322	-5.49	1.46	-0.14	3.23	1.22E-08	1.28E-15
Skipwith Pond	33	0.4848	-5.01	1.32	-0.81	0.89	2.69E-08	1.22E-15
Broadstone Stream	29	0.3200	-6.85	1.04	-1.07	1.35	5.75E-10	9.73E-19
UK Grasslands	61	0.0608	-5.00	2.10	0.56	2.31	2.11E-09	8.04E-18
Gearagh Woodland	113	0.0580	-5.31	4.46	-0.17	5.05	2.79E-09	5.88E-17
Estero de Punta Banda	119	0.1534	-2.58	6.67	-2.28	6.63	9.44E-06	4.72E-10

669